ChemComm

COMMUNICATION

View Article Online
View Journal | View Issue

Check for updates

Cite this: *Chem. Commun.*, 2017, **53**, 9008

Received 2nd May 2017,
Accepted 20th July 2017

DOI: 10.1039/c7cc02638b

rsc.li/chemcomm

Phosphorescent 2-, 3- and 4-coordinate cyclic (alkyl)(amino)carbene (CAAC) Cu(I) complexes†

Rasha Hamze,[a] Rodolphe Jazzar,[b] Michele Soleilhavoup,[b] Peter I. Djurovich,[a] Guy Bertrand[b] and Mark E. Thompson*[a]

The photophysical properties of several Cu(I) complexes coordinated with cyclic (alkyl)(amino)carbene (CAAC) ligands were examined. All the compounds were found to be phosphorescent, regardless of whether they are 2-, 3- or 4-coordinated. Aggregate and excimer emission were observed from 2-coordinate CAAC–CuCl derivatives in methylcyclohexane solution. Emission from the complex 4-coordinated with a trispyrazolylborate ligand is red-shifted with respect to both the chloro-derivative and an analogous complex with an NHC ligand.

Luminescent copper(I) complexes have been employed in applications ranging from organic light emitting diodes (OLEDs)[1] and downconverters[2] to sensors.[3] Such applications take advantage of the excited triplet state, which is utilized either directly through phosphorescence[4] or indirectly *via* thermally-activated delayed fluorescence (TADF).[1a,5] As such, developing paradigms for tuning the chemical and electronic properties of Cu(I) luminophores is of increasing importance. However, the set of ligands used has been traditionally limited to bidentate, chelating N^N,[6] P^P,[7] N^P,[8] and mixtures of both N^N and P^P type ligands,[9] as well as different halides.[4,10] Color tuning in these systems is typically achieved by incorporating electron-donating or withdrawing groups and aza-substitutions onto the ligands supporting the frontier orbitals[2,11] as well as increasing the size of the chromophoric ligand.[10b,12] More recently, N-heterocyclic carbenes (NHCs) have emerged as a class of chromophoric ligands for Cu(I) complexes[13] with desirable properties such as strong metal–carbon bonds and amenability to color-tuning through chemical modification of the carbene itself.[13b] Here too, ligand modifications such as benzannulation and aza-substitution of imidazole-based NHCs were used to shift the emission energies to longer wavelengths.[13b] These modifications were aimed at stabilizing the chromophoric, carbene-based LUMO, that leads to increased contribution from the vacant $2p_z$ orbital on the carbene carbon. With this knowledge, we turned our attention to cyclic (alkyl)(amino)carbenes (CAACs) as an alternate class of highly electrophilic carbenes,[14] known for their superior π-accepting and σ-donating properties compared to NHCs.[15] Over the past year alone, three literature accounts have highlighted the chromophoric properties of CAAC–CuCl complexes.[16] In two separate accounts, Romanov, Bochmann *et al.* reported that emission from CAAC–CuCl complexes was exclusively from prompt fluorescence, with subnanosecond[16a] and nanosecond[16c] lifetimes. Such poor intersystem crossing and subsequent absence of phosphorescence is highly unusual in luminescent Cu(I) complexes. Furthermore, the aforementioned results are not in agreement with data obtained by Gernert *et al.*, who reported typical microsecond lifetimes for similar complexes.[16b] In this work, we first re-examine the photophysical properties of two previously reported 2-coordinate CAAC–CuCl complexes, **1-Cl** and **2-Cl**, in different media and find no evidence for prompt emission. Second, we employed trispyrazolylborate, Tp, as an anionic chelating ligand with higher hapticity than chloride. The resultant complexes, **1-Tp** and **2-Tp**, have 4- and 3-coordinate geometry, respectively, around the metal centre. An analogous NHC-complex, **3-Tp**, was prepared and used as a reference (Fig. 1).

Complexes **1-Cl** and **2-Cl** were synthesized following reported literature procedures.[16a,17] In the case of the less sterically encumbered **1-Cl**, we found that the complex disproportionates over time in a polar, coordinating solvent such as THF, into the symmetric metathesis product, $[(CAAC)_2Cu]^+$, $CuCl_2^-$. This type of disproportionation has previously been observed in Cu–NHC complexes.[18] It is noteworthy that $[(CAAC)_2Cu]^+$ is also formed as a byproduct during the reaction leading to CAAC–CuCl, and the two complexes precipitate together. The $[(CAAC)_2Cu]^+$ complex has distinct spectral features (narrow, structured emission),[16b] that can cause errors in photophysical measurements. Slow recrystallization under

---

[a] *Department of Chemistry, University of Southern California, Los Angeles, 90089, California, USA. E-mail: met@usc.edu*

[b] *Department of Chemistry, University of California, San Diego, La Jolla, 92093, California, USA*

† Electronic supplementary information (ESI) available: Details of experimental procedures, spectroscopic and calculation data. CCDC 1541973, 1541974, and 1541975 for **1-Tp**, **2-Tp** and **3-Tp** respectively. For ESI and crystallographic data in CIF or other electronic format see DOI: 10.1039/c7cc02638b

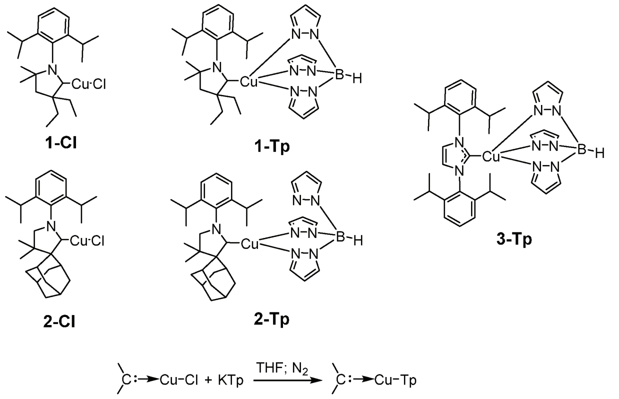

Fig. 1 CAAC–Cu chlorides and trispyrazolylborates (Tp) used in this work. Also shown is the synthetic scheme for the Tp complexes.

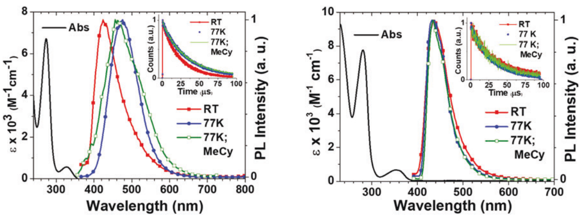

Fig. 2 Absorption in CH_2Cl_2 (black trace) and emission spectra of **1-Cl** (left) and **2-Cl** (right) as neat solids (red and blue traces, closed symbols) and in frozen methylcyclohexane (MeCy) solution (green trace, open squares). The insets show the PL decay transients of the neat solids recorded at room temperature (red) and 77 K (blue) and in frozen MeCy solution (green).

an inert atmosphere allowed for successful separation of the two compounds. X-ray diffraction analyses of single crystals obtained therein confirmed the reported two-coordinate structure. Fig. 2 shows the absorption (in dichloromethane) and emission spectra (solid state and in frozen solution) for **1-Cl** and **2-Cl**. Weak, low-lying absorption bands ($\lambda_{\max} = 328$ nm, $\varepsilon = 1.4 \times 10^3$ M^{-1} cm^{-1} for **1-Cl** and $\lambda_{\max} = 352$ nm, $\varepsilon = 6 \times 10^2$ M^{-1} cm^{-1} for **2-Cl**; Table 1) tentatively assigned to singlet XMLCT transitions,[19] are in agreement with spectra reported earlier.[16] As described by Romanov *et al.*,[16a,c] both chloro-complexes have high luminescent quantum yields (Φ) in their crystalline and powder form, and exhibit broad and featureless emission profiles indicative of a CT nature for the emissive state ($\lambda_{\max} = 424$ nm; $\Phi = 0.86$ for **1-Cl** and $\lambda_{\max} = 436$ nm; $\Phi = 0.96$ for **2-Cl**). The excited state lifetimes show monoexponential decays ($\tau = 22$ μs for **1-Cl** and 29 μs for **2-Cl**, Table 1), indicating that the origin of luminescence in both complexes is phosphorescence (insets in Fig. 2). The radiative rate constants for **1-Cl** and **2-Cl**, ($k_r = 3.9 \times 10^4$ s^{-1} and 3.3×10^4 s^{-1}, respectively) (Table 1), are comparable to those in NHC–Cu complexes[13a,b] and to the CAAC–Cu complexes reported by Gernert *et al.*[16b] Furthermore, the experimental k_r values for both complexes are in agreement with the theoretical values obtained from the Strickler–Berg relation[20] using the extinction coefficients for the lowest energy transitions.

The microsecond lifetimes we find for emission are in contrast with the report by Romanov *et al.*, who reported lifetimes of 0.2–0.3 ns for **2-Cl**[16a] and 3.2 ns for **1-Cl**.[16c] The unusually fast signal given in the former study likely stems from the instrument response function (irf), which the authors note to have a width of 0.2 ns, nearly identical to the reported lifetime of **2-Cl** and its bromo- and iodo-analogues.[16a] In their investigation of the luminescence of **1-Cl**, the authors also recorded a long-lived component with a decay lifetime of 25.7 μs,[16c] which they attributed to a photodecomposition product. We observed similar decay lifetimes in both crystalline ($\tau = 22$ μs; Table 1) and fine powder ($\tau = 23$ μs; Fig. S9, ESI†) forms of **1-Cl**, which lead us to conclude that this value is the true excited state lifetime of the phosphorescent complex. Moreover, we observed that luminescence from solid **2-Cl** is independent of temperature; the lifetime and emission profiles are virtually unchanged at 77 K ($\tau = 28$ μs, $\lambda_{\max} = 432$ nm; Table 1). Interestingly, **1-Cl** shows a pronounced red-shift in emission at 77 K ($\Delta\lambda_{\max} = 52$ nm). However, since this shift is not accompanied by a significant increase in excited state lifetimes ($\tau = 22$ μs at RT and 32 μs at 77 K), TADF is ruled unlikely, and the red-shift is attributed to changes in the solid-state packing upon cooling. To confirm that the photophysical properties measured for these samples correspond to the pure complexes and not to photodecomposition products, ^{1}H-NMR and UV-visible spectra of the solid and dissolved samples were recorded after photophysical characterization (including irradiation at $\lambda = 281$ nm, 305 nm, and 331 nm). The resultant data showed no signs of decomposition products (Fig. S9, S10, S20 and S21, ESI†).

UV-visible absorption spectra of the two chloride complexes obtained in solutions of methylcyclohexane (MeCy), 2-methyltetrahydrofuran (2-MeTHF) and dichloromethane show negative solvatochromism (Fig. S8, ESI†). Luminescent spectra of both **1-Cl** and **2-Cl** at room temperature in 2-MeTHF, a good coordinating solvent, show orange phosphorescence that is independent of concentration (Fig. S4 and S5, ESI†). As reported by Romanov *et al.*,[16a] this shift in emission energy is likely due to exciplex

Table 1 Photophysical data for complexes **1-** and **2-Cl**, and **1-**, **2-** and **3-Tp**

	Absorbance, λ (nm) ε (10^3 M^{-1} cm^{-1})^a	Emission at room temperature^b					Emission at 77 K^b	
		$\lambda_{\max}$ (nm)	τ (μs)	Φ	k_r (s^{-1})	k_{nr} (s^{-1})	$\lambda_{\max}$ (nm)	τ (μs)
1-Cl	269 (9.2), 328 (1.4)	424	22	0.86	3.9×10^4	6.4×10^3	476	32
2-Cl	281 (7.8), 352 (0.6)	436	29	0.96	3.3×10^4	1.4×10^3	432	28
1-Tp	278 (7.7), 336 (3.4)	550	12	0.46	3.9×10^4	4.6×10^4	562	9.6 (20%), 24 (80%)
2-Tp	310 (4.8), 348 sh (2.1)	616	0.4 (40%), 1.0 (60%)	0.02	$2.6 \times 10^{4\,c}$	$1.3 \times 10^{6\,c}$	614	4.2 (75%), 14 (25%)
3-Tp	207 (17), 299 (6.0)	468	29	0.25	8.6×10^3	2.6×10^4	468	21

[a] In dichloromethane. [b] In solid state. [c] Calculated from the weighted average of the two contributions to τ.

formation. Such excited state interactions do not occur in frozen 2-MeTHF, and both complexes regain blue emission and long lifetimes consistent with their behaviour in the solid state (Table S8, ESI†). Interestingly, solutions of **1-Cl** and **2-Cl** in non-coordinating MeCy exhibit concentration-dependent emission with two peaks: one blue peak, similar to the solid state ($\lambda_{\max}$ = 442 nm for **1-Cl** and 476 nm for **2-Cl**), and the other peak red-shifted ($\lambda_{\max}$ = 570 nm for **1-Cl** and 614 nm for **2-Cl**; Fig. 3 and Fig. S7, ESI†); an observation which is indicative of aggregate formation. This is verified upon dilution, as the intensity of the low energy band is reduced relative to the peak at higher energy, whereas the absorption spectra remain unchanged (Fig. 3 for **1-Cl**). Furthermore, the excited state decays recorded for the band at low energy in **2-Cl** display a rise time that is concentration-dependent. (Fig. 3, inset and Table S8, ESI†). Congruently, the low energy emission is less intense in **2-Cl** than in **1-Cl**, likely due to the steric bulk in the former complex hindering aggregate formation (Fig. S7, ESI†). Orange-coloured, μ-bridging chloride dimers of analogous diamidocarbene (DAC) copper–chloride complexes have been isolated by Collins *et al.*[21] A similar type of dimer formed in the ground state for **1-Cl** and excited state for **2-Cl** might be responsible for the low energy emission observed in MeCy solution. The excimer formation in **2-Cl** is diffusion limited in MeCy, with the formation rate constant $k_f^E = 7.4 \times 10^9\ s^{-1}$ (Fig. S15, ESI†).

To further investigate the luminescence properties of the CAAC–Cu complexes, the Tp ligand was incorporated for its stronger σ-donating properties than –Cl, and its ability to afford luminescent M(I) complexes.[22] Simple addition of a stoichiometric amount of potassium trispyrazolylborate (KTp) to the carbene–CuCl precursors in THF yielded complexes **1-Tp** and **2-Tp** in high yields (Fig. 1). **1-Tp** was also isolated from the cationic $[(CAAC)_2Cu]^+$, $CuCl_2^-$ following the same method, showing that the anionic Tp ligand can displace the carbene. The isolated yellow-orange powders have moderate stability in air, and are less stable in aerated solution, decomposing over a few hours to several days. X-ray analysis of single crystals showed that while complex **1-Tp** is four-coordinate around the Cu center, **2-Tp** is 3-coordinate in its crystalline matrix, likely due to the steric demands of the bulky adamantyl substituent. The two complexes have similar Cu–C$_{carbene}$ bond lengths at 1.904(1) Å for **1-Cl** and 1.886(1) Å for **2-Cl.** The tridentate ligand in **1-Tp** binds in a typical scorpionate fashion, with one pyrazole (pz) ring chelated at a slightly longer bond distance (Cu–N = 2.151(1) Å) than the other two (Cu–N = 2.123(1) Å and 2.138(1) Å). In the bulkier **2-Tp**, the third, pendant pz ring lies twisted and uncoordinated from the metal center (Cu–N = 3.655(2) Å). The bond lengths for the two coordinated pz rings are shorter than those in **1-Tp** (Cu–N = 1.970(1) Å and 2.053(1) Å). Despite the asymmetric binding nature of Tp in both complexes, and the asymmetry of the CAAC ligand itself, ^{1}H NMR spectra of both complexes show only three resonances corresponding to the three unique protons on the pz rings. This pattern is characteristic of *C*3 symmetry, indicating equilibration of all three groups on the NMR time scale at room temperature. An underlying mechanism for this behavior was proposed by Trofimenko in 1969,[23] and likely involves the dissociation of a pz group, as suggested by the structure of **2-Tp**, followed by rotation of the carbene ligand. Further investigation of the dynamic behavior of carbene–Cu-Tp complexes is ongoing.

The UV-visible absorption spectra of both **1-Tp** and **2-Tp** in dichloromethane are shown in Fig. 4. Absorption cut-offs for these complexes are red-shifted with respect to their chloride precursors: 460 nm for **1-Tp** and 480 nm for **2-Tp**, compared with 370 nm and 400 nm for 1- and **2-Cl** respectively. Upon photoexcitation, crystals of **1-Tp** exhibit bright yellow phosphorescence ($\lambda_{\max}$ = 550 nm, τ = 12 μs, Φ = 0.46). On the other hand, crystals of the 3-coordinate **2-Tp** display weak orange phosphorescence ($\lambda_{\max}$ = 616 nm, Φ = 0.02). Accordingly, its excited state is short-lived and exhibits biexponential decay (τ_1 = 0.4 μs, 40%; τ_2 = 1.0 μs, 60%). However, upon cooling the sample down to 77 K, the excited state lifetime of the complex increases (τ_1 = 4.2 μs, 75%; τ_2 = 14 μs, 25%), concomitant with an increase in the luminescence intensity (Fig. S11, ESI†).

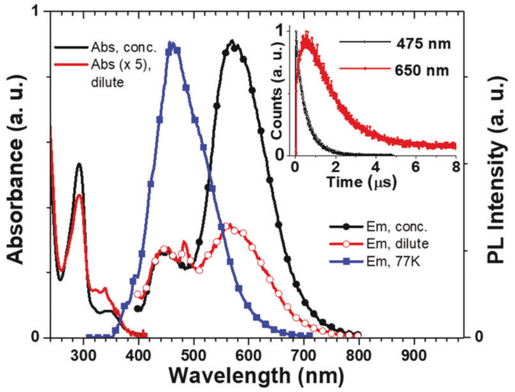

Fig. 3 Absorption (dashed lines) and emission (solid lines, symbols) of concentrated (6.8 × 10^{-5} M; black) and 5-fold dilute (red) solutions of **1-Cl** in MeCy at room temperature, as well as of the frozen solution (blue line). Inset: PL transients measured in a concentrated solution of **2-Cl** in MeCy, showing the decay of the band at high energy (τ = 0.54 μs) coincident with the rise (τ = 0.42 μs) and fall (τ = 1.34 μs) of the transient from the low-energy emission band.

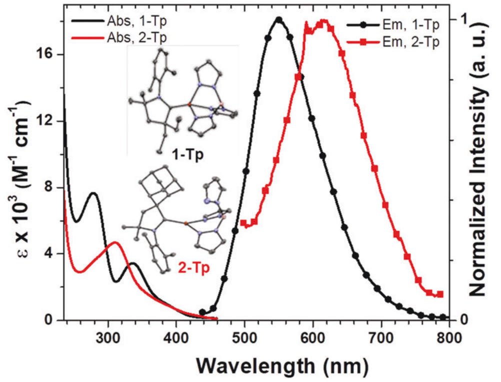

Fig. 4 Absorption spectra of **1-Tp** (black) and **2-Tp** (red) in CH_2Cl_2 (dashed lines) and emission spectra of the microcrystalline solids (solid lines with symbols). Also shown are the x-ray structures of the complexes.

This change reflects an incomplete suppression of the molecular distortions responsible for non-radiative decay upon cooling. The dramatic variation in PLQY between the two CAAC–CuTp complexes highlights the impact of hapticity of the Tp ligand on rate of non-radiative decay.

Computational analyses of the ground state properties of **1-Tp** and **2-Tp** were performed using DFT calculations at the B3LYP, LACVP** level. The two complexes share similar frontier orbital contributions, with the HOMO being principally Cu-based, and the LUMO being largely localized on the empty p_z orbital on the carbene carbon as well as the electron-withdrawing nitrogen of the CAAC ring (Table S10, ESI†). The optimized T_1 geometry for **1-Tp** shows minimal change from the ground state structure, whereas **2-Tp** undergoes a pronounced Y-to-T distortion.[24] The spin density resides primarily over the Cu–C carbene atoms for both complexes (Table S10, ESI†). The T_1 energies calculated by either TDDFT or difference in optimized S_0 and T_1 geometries (ΔSCF) compare favorably to the experimental emission values (TDDFT: T_1 = 432 nm for **1-Tp** and 461 nm for **2-Tp**; ΔSCF = 497 nm for **1-Tp** and 503 nm for **2-Tp**). In both complexes, the calculated singlet–triplet gap (ΔE_{S1-T1} = 480 meV for **1-Tp** and 580 meV for **2-Tp**) is too large for TADF at room temperature.[5]

Finally, to determine the extent to which emission is red-shifted by the electrophilic CAAC ligand relative to an NHC–Cu complex, we prepared **3-Tp** featuring an imidazolylidene ring as the NHC ligand (Fig. 1). Microcrystals of the 4-coordinate complex (Fig. S12, ESI†) exhibited blue, temperature-independent phosphorescence (λ_{max} = 468 nm, τ = 29 μs, Φ = 0.25). The red-shift in phosphorescence observed between **1-Tp** and **3-Tp** (82 nm, 0.40 eV) agrees with the DFT calculations that show a significant stabilization of the LUMO in the CAAC complex relative to the NHC derivative (E_{LUMO} = −0.74 eV for **1-Tp** and −0.37 eV for **3-Tp**, Table S10, ESI†).

In conclusion, we report a series of 2-, 3- and 4-coordinate CAAC–Cu complexes utilizing either chloride or trispyrazolylborate as ancillary ligands. The radiative rate constants for all the complexes are similar (k_r = 2.6–3.9 × 10^4 s^{-1}) indicative of emission from the triplet state. In non-coordinating MeCy, the chloro-derivatives display concentration-dependent, orange emission consistent with dimer and excimer formation for **1-Cl** and **2-Cl**, respectively. This effect is more pronounced in the case of the less sterically encumbered **1-Cl**. Upon displacement of the chloride with Tp, 4- and 3-coordinate complexes are obtained (**1-Tp** and **2-Tp** respectively), that exhibit yellow to orange phosphorescence, with the 4-coordinate **1-Tp** being more efficient than the 3-coordinate **2-Tp**. The emission energies in both CAAC–Cu complexes are red-shifted relative to an NHC–Cu analogue. These attributes make CAACs a highly-promising ligand set for attaining efficient, yellow and orange phosphorescence.

The authors like to thank the Universal Display Corporation and NSF (CHE-1359809) for generous financial support of this work.

Notes and references

1 (*a*) J. C. Deaton, S. C. Switalski, D. Y. Kondakov, R. H. Young, T. D. Pawlik, D. J. Giesen, S. B. Harkins, A. J. M. Miller, S. F. Mickenberg and J. C. Peters, *J. Am. Chem. Soc.*, 2010, **132**, 9499–9508; (*b*) Z. Liu, M. F. Qayyum, C. Wu, M. T. Whited, P. I. Djurovich, K. O. Hodgson, B. Hedman, E. I. Solomon and M. E. Thompson, *J. Am. Chem. Soc.*, 2011, **133**, 3700–3703.

2 W. Liu, Y. Fang, G. Z. Wei, S. J. Teat, K. Xiong, Z. Hu, W. P. Lustig and J. Li, *J. Am. Chem. Soc.*, 2015, **137**, 9400–9408.

3 (*a*) C. S. Smith, C. W. Branham, B. J. Marquardt and K. R. Mann, *J. Am. Chem. Soc.*, 2010, **132**, 14079–14085; (*b*) X.-Y. Xu, H.-N. Xiao and A.-P. Deng, *Opt. Mater.*, 2014, **36**, 1542–1554.

4 M. Hashimoto, S. Igawa, M. Yashima, I. Kawata, M. Hoshino and M. Osawa, *J. Am. Chem. Soc.*, 2011, **133**, 10348–10351.

5 R. Czerwieniec, M. J. Leitl, H. H. H. Homeier and H. Yersin, *Coord. Chem. Rev.*, 2016, **325**, 2–28.

6 D. G. Cuttell, S.-M. Kuang, P. E. Fanwick, D. R. McMillin and R. A. Walton, *J. Am. Chem. Soc.*, 2002, **124**, 6–7.

7 (*a*) R. Czerwieniec, K. Kowalski and H. Yersin, *Dalton Trans.*, 2013, **42**, 9826–9830; (*b*) M. Osawa, I. Kawata, R. Ishii, S. Igawa, M. Hashimoto and M. Hoshino, *J. Mater. Chem. C*, 2013, **1**, 4375–4383.

8 T. Hofbeck, U. Monkowius and H. Yersin, *J. Am. Chem. Soc.*, 2015, **137**, 399–404.

9 C. L. Linfoot, M. J. Leitl, P. Richardson, A. F. Rausch, O. Chepelin, F. J. White, H. Yersin and N. Robertson, *Inorg. Chem.*, 2014, **53**, 10854–10861.

10 (*a*) X. Zhang, L. Song, M. Hong, H. Shi, K. Xu, Q. Lin, Y. Zhao, Y. Tian, J. Sun, K. Shu and W. Chai, *Polyhedron*, 2014, **81**, 687–694; (*b*) N. M. Khatri, M. H. Pablico-Lansigan, W. L. Boncher, J. E. Mertzman, A. C. Labatete, L. M. Grande, D. Wunder, M. J. Prushan, W. Zhang, P. S. Halasyamani, J. H. S. K. Monteiro, A. D. Bettencourt-Dias and S. L. Stoll, *Inorg. Chem.*, 2016, **55**, 11408–11417.

11 (*a*) Z. Liu, P. I. Djurovich, M. T. Whited and M. E. Thompson, *Inorg. Chem.*, 2012, **51**, 230–236; (*b*) K. J. Lotito and J. C. Peters, *Chem. Commun.*, 2010, **46**, 3690–3692; (*c*) F. Wei, J. Qiu, X. Liu, J. Wang, H. Wei, Z. Wang, Z. Liu, Z. Bian, Z. Lu, Y. Zhao and C. Huang, *J. Mater. Chem. C*, 2014, **2**, 6333–6341.

12 T. Ni, X. Liu, T. Zhang, H. Bao, G. Zhan, N. Jiang, J. Wang, Z. Liu, Z. Bian, Z. Lu and C. Huang, *J. Mater. Chem. C*, 2015, **3**, 5835–5843.

13 (*a*) V. A. Krylova, P. I. Djurovich, M. T. Whited and M. E. Thompson, *Chem. Commun.*, 2010, **46**, 6696–6698; (*b*) V. A. Krylova, P. I. Djurovich, B. L. Conley, R. Haiges, M. T. Whited, T. J. Williams and M. E. Thompson, *Chem. Commun.*, 2014, **50**, 7176–7179; (*c*) R. Marion, F. Sguerra, F. Di Meo, E. Sauvageot, J.-F. Lohier, R. Daniellou, J.-L. Renaud, M. Linares, M. Hamel and S. Gaillard, *Inorg. Chem.*, 2014, **53**, 9181–9191.

14 (*a*) O. Back, M. Henry-Ellinger, C. D. Martin, D. Martin and G. Bertrand, *Angew. Chem., Int. Ed.*, 2013, **52**, 2939–2943; (*b*) M. Soleilhavoup and G. Bertrand, *Acc. Chem. Res.*, 2015, **48**, 256–266; (*c*) V. Lavallo, Y. Canac, C. Prasang, B. Donnadieu and G. Bertrand, *Angew. Chem., Int. Ed.*, 2005, **44**, 5705–5709.

15 B. Rao, H. R. Tang, X. M. Zeng, L. Liu, M. Melaimi and G. Bertrand, *Angew. Chem., Int. Ed.*, 2015, **54**, 14915–14919.

16 (*a*) A. S. Romanov, D. Di, L. Yang, J. Fernandez-Cestau, C. R. Becker, C. E. James, B. Zhu, M. Linnolahti, D. Credgington and M. Bochmann, *Chem. Commun.*, 2016, **52**, 6379–6382; (*b*) M. Gernert, U. Müller, M. Haehnel, J. Pflaum and A. Steffen, *Chem. – Eur. J.*, 2017, **23**, 2206–2216; (*c*) M. Bochmann, A. S. Romanov, C. R. Becker, C. E. James, D. Di, D. Credgington and M. Linnolahti, *Chem. – Eur. J.*, 2017, **23**, 4625–4637.

17 (*a*) X. B. Hu, M. Soleilhavoup, M. Melaimi, J. X. Chu and G. Bertrand, *Angew. Chem., Int. Ed.*, 2015, **54**, 6008–6011; (*b*) G. D. Frey, R. D. Dewhurst, S. Kousar, B. Donnadieu and G. Bertrand, *J. Organomet. Chem.*, 2008, **693**, 1674–1682.

18 E. Alvarado, A. C. Badaj, T. G. Larocque and G. G. Lavoie, *Chem. – Eur. J.*, 2012, **18**, 12112–12121.

19 (*a*) P. C. Ford, E. Cariati and J. Bourassa, *Chem. Rev.*, 1999, **99**, 3625–3647; (*b*) V. W. W. Yam and K. K. W. Lo, *Chem. Soc. Rev.*, 1999, **28**, 323–334; (*c*) H. D. Hardt and A. Pierre, *Z. Anorg. Allg. Chem.*, 1973, **402**, 107–112; (*d*) P. C. Ford and A. Vogler, *Acc. Chem. Res.*, 1993, **26**, 220–226.

20 S. J. Strickler and R. A. Berg, *J. Chem. Phys.*, 1962, **37**, 814–822.

21 L. R. Collins, J. P. Lowe, M. F. Mahon, R. C. Poulten and M. K. Whittlesey, *Inorg. Chem.*, 2014, **53**, 2699–2707.

22 (*a*) A. Acosta, J. I. Zink and J. Cheon, *Inorg. Chem.*, 2000, **39**, 427–432; (*b*) H. Kunkely, V. Pawlowski, A. Strasser and A. Vogler, *Inorg. Chem. Commun.*, 2008, **11**, 415–417.

23 S. Trofimenko, *J. Am. Chem. Soc.*, 1969, **91**, 3183–3189.

24 K. A. Barakat, T. R. Cundari and M. A. Omary, *J. Am. Chem. Soc.*, 2003, **125**, 14228–14229.